19th Brazilian Congress of Thermal Sciences and Engineering
November 6th–10th, 2022, Bento Gonçalves - RS - Brazil

# ENC-2022-0279
# REAL-TIME INTERNAL HEAT FLUX ESTIMATION ON PULSATING HEAT PIPES USING KALMAN FILTER

**Bruno Henrique Marques Margotto**
**Carlos Eduardo Polatschek Kopperschmidt**
**Marcelo José Colaço**
brunohmmargotto@mecanica.coppe.ufrj.br
cadupolkop@mecanica.coppe.ufrj.br
colaco@mecanica.coppe.ufrj.br
Federal University of Rio de Janeiro, UFRJ. Technology Center, Av. Athnos da Silveira Ramos, 149 - Bloco A, 2 andar – Cidade Universitária da UFRJ, Ilha do Governador, Rio de Janeiro/RJ, 21.941-909.

**Wellington Betencurte da Silva**
**Julio Cesar Sampaio Dutra**
wellinton.betencurte@ufes.br
julio.dutra@ufes.br
Federal University of Espírito Santo, UFES. Alto Universitário, s/n, Guararema, Alegre/ES, 29.500-999.

**Luca Pagliarini**
**Luca Cattani**
**Fabio Bozzoli**
luca.pagliarini@studenti.unipr.it
luca.cattani1@unipr.it
fabio.bozzoli@unipr.it
Department of Engineering and Architecture, University of Parma, Parco Area delle Scienze 181/A, Parma, Italy

***Abstract.*** *In this paper, we use the Kalman filter to estimate the internal heat flux between a working fluid and the tube wall along the adiabatic section of a Pulsating Heat Pipe device by considering available the temperature measurement on the external surface. The current study is attractive due to the possibility of real-time evaluation of heat fluxes, which provides important information regarding the operation conditions for such devices. The temperature measurement was obtained by solving the transient 1D heat conduction problem, simulating the data acquisition which could be made by an Infrared Camera. The Kalman filter estimation accuracy was analysed by considering different values of measurement noises and heat flux functions. Also, the Tikhonov Regularization was crucial to reduce instabilities on the heat flux estimation in all measurement noises. The results were obtained with good agreement with the exact data, showing a promising technique for real-time evaluation of thermal behaviour on such thermal devices.*

***Keywords:*** *Pulsating Heat Pipes, Inverse Heat Transfer Problem, Kalman Filter, Two-phase Flow*

## 1. INTRODUCTION

The advances in electronics and aerospace technology allowed the development of advanced equipment with massive computational power. These devices, however, require a high amount of heat to be removed, in order to maintain their temperature within a desired range and guarantee their correct working condition. One solution for cooling such devices are the Pulsating Heat Pipes, passive two-phase heat transfer devices characterized by the oscillating movement of the working fluid, which are able to work without external electrical energy and having high heat transfer capacity (Bastakoti *et al.*, 2018). Also, its working principle allows their use on absence of gravity, being of great interest for the aerospace engineering applications (Marengo and Nikolayev, 2018).

According to Han *et al.* (2016), these devices are thermically characterized in terms of their global performance through an equivalent thermal resistance. Nevertheless, a better and precise comprehension of the working principles

of PHP devices is necessary concerning the local heat transfer evaluation between the working fluid and the PHP inner wall (Pagliarini *et al.*, 2021). Recent works, e.g. Cattani *et al.* (2019) and Pagliarini *et al.* (2021), propose the estimation of local heat flux using different techniques for inverse problem solution, which allow a better comprehension of its working principle. Therefore, the real-time estimation of the heat flux on these thermal devices is very attractive to obtain more precisely information of their thermal behaviour and, consequently, the flow pattern during operation. For this purpose Bayesian filters, commonly used on tracking problems (Ristic *et al.*, 2004), are very attractive, since such techniques have been used to solve Inverse Heat Conduction Problems for parameter estimation, e.g. Daouas and Radhouani (2000); Orlande *et al.* (2008, 2012); Pacheco *et al.* (2014); Wang *et al.* (2020) and their applications are relatively simple implementation with low computational costs, allowing their use for real-time applications.

In the current paper, our goal is to evaluate the Kalman filter capability to achieve the real-time heat flux estimation on Pulsating Heat Pipes. The heat flux estimation is performed by solving an Inverse Heat Conduction Problem to estimate the local heat flux with Kalman filter. The mathematical modeling for the direct problem was based on Pagliarini *et al.* (2021). The measurement acquisition is assumed to be made by an Infrared Camera in the real case, while in this paper it was obtained by solving a forward transient 1D heat conduction problem. The internal heat flux varies with space and time, reproducing the thermal behaviour of the two-phase flow inside the tube. Different heat flux function were considered to assess the Kalman filter performance on estimation. Also, different measurement noise levels are considered to evaluate the filter accuracy for the proposed heat flux functions.

## 2. FORWARD PROBLEM

The physical problem is defined as a heat conduction problem, where the studied domain is the adiabatic section of a PHP device. We consider on the inner tube surface the heat flux exchange between the tube wall and working fluid, here represented as a time-space function $q\,(z,t)$, and on the outer surface the heat exchanged between the tube wall and the environment, considering $T_\infty$ the environment temperature and $h_\infty$ the convection heat transfer coefficient. We follow therefore assuming the inner and outer radius are $r_\mathrm{i}$ and $r_\mathrm{o}$, respectively. The studied section of the tube has length of $L$. We present a scheme for the described heat conduction problem in Fig. 1. Here, we consider that the temperature does not change on the angular component.

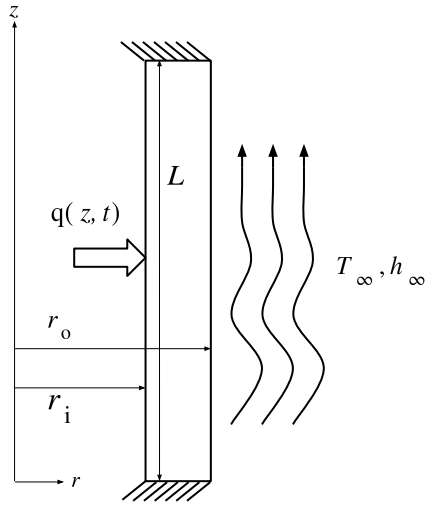


Figure 1. Representation of PHP wall domain.

We assume the thin-wall approach for the heat conduction problem (Pagliarini *et al.*, 2021), reducing the 2D problem to an 1D problem. Thus, we are able to write the mathematical formulation for the heat conduction problem by Eqs. (1) - (5).

$$\frac{1}{\alpha}\frac{\partial T}{\partial t} = \frac{\partial^2 T}{\partial z^2} + C_1 q\,(z,t) + C_2\,T + C_3 \tag{1}$$

$$\left.\frac{\partial T}{\partial z}\right|_{z=0} = \left.\frac{\partial T}{\partial z}\right|_{z=L} = 0 \tag{2}$$

Where:

$$C_1 = \frac{2r_i}{k\left(r_o^2 - r_i^2\right)} \tag{3}$$

$$C_2 = -\frac{2h_\infty r_o}{k\left(r_o^2 - r_i^2\right)} \tag{4}$$

$$C_3 = \frac{2h_\infty r_o T_\infty}{k\left(r_o^2 - r_i^2\right)} \tag{5}$$

The solution of Eqs. (1) and (2) provide the temperature field on the PHP wall domain by solving these equations by the Explicit Finite Difference Method (Özisik *et al.*, 2017), considering k the index for the present instant and $\Delta t$ the time-step between the instants k and k $-$ 1. Thus, we can obtain the temperature for the next time step by Eq. (6).

$$\mathbf{T}^{\mathrm{k}} = \mathbf{J}\mathbf{T}^{\mathrm{k}-1} + \mathbf{s}^{\mathrm{k}-1} \tag{6}$$

Where **J** and **S** are the matrices obtained from the discretization and **T** is the vector containing the temperature nodes. We consider $M$ and $\Delta z$ the total nodes for space discretization and the distance between nodes, respectively, allowing **J**, **S** and **T** to be build by Eq. (7) - (10). We should note that $r_z$, defined in Eq. (10), is a crucial parameter to guarantee the stability of the explicit scheme, which requires that its value be less than 0.5 (Özisik *et al.*, 2017).

$$\mathbf{J} = \begin{bmatrix} (1-2r_z+\alpha\Delta t C_2) & 2r_z & 0 & \dots & 0 & 0 & 0 \\ r_z & 1-2r_z+\alpha\Delta t C_2 & r_z & \dots & 0 & 0 & 0 \\ \vdots & \vdots & \vdots & \ddots & \vdots & \vdots & \vdots \\ 0 & 0 & 0 & \dots & r_z & 1-2r_z+\alpha\Delta t C_2 & r_z \\ 0 & 0 & 0 & \dots & 0 & 2r_z & (1-2r_z+\alpha\Delta t C_2) \end{bmatrix} \tag{7}$$

$$\mathbf{s}^{\mathrm{k}-1} = \alpha\Delta t \begin{bmatrix} C_1 q\left(z_1, t_{\mathrm{k}-1}\right) + C_3 \\ C_1 q\left(z_2, t_{\mathrm{k}-1}\right) + C_3 \\ \vdots \\ C_1 q\left(z_{M-1}, t_{\mathrm{k}-1}\right) + C_3 \\ C_1 q\left(z_M, t_{\mathrm{k}-1}\right) + C_3 \end{bmatrix} \tag{8}$$

$$\mathbf{T}^{\mathrm{k}} = \begin{bmatrix} T_1^{\mathrm{k}} \\ T_2^{\mathrm{k}} \\ \vdots \\ T_{M-1}^{\mathrm{k}} \\ T_M^{\mathrm{k}} \end{bmatrix} \tag{9}$$

$$r_z = \frac{\alpha\Delta t}{\Delta z} \tag{10}$$

## 3. INVERSE PROBLEM

The heat flux estimation on the inner surface of the tube wall is achieved by the solution of the Inverse Heat Conduction Problem (IHCP). In this paper we apply the Kalman filter to solve the inverse problem by state (temperature) and parameter (heat flux) estimation. The Kalman filter is an optimal recursive estimator based on Bayesian inference for linear problems and Gaussian errors involved, computing sequentially the *posterior* density function for the estimated state when measurements are available, allowing the estimation of unobservable states (Ristic *et al.*, 2004).

In this work, the estimation problem is defined as a *filtering problem* (Kaipio and Somersalo, 2004), which consists on two basic steps: *Prediction* and *Update*. With the *priori information* available, the states for the next instant are calculated by the *Evolution model* (prediction step) and, when the measurements are available, represented by *Observation model*, the states are corrected by Kalman filter equations (update step). This procedure is repeated sequentially until the end of time experiment and is presented in Fig. 2. Hence, consider the state vector at instant k as $\mathbf{x}_{\mathrm{k}}$, which contains all state variables involved on the estimation problem (in this case it will be composed by the temperature and heat flux information), and $\mathbf{y}_{\mathrm{k}}$ is the measurement vector at instant k, which contains the observable states, in this case the temperature field. We consider uncorrelated white-Gaussian random sequences $\mathbf{w}_{\mathrm{k\text{-}1}}$ and $\mathbf{v}_{\mathrm{k\text{-}1}}$, $\mathbf{Q}_{\mathrm{k}}$ and $\mathbf{R}_k$, as the noises for Evolution and Observation models, respectively. So, the pair *Evolution-Observation* model is written as a stochastic-discrete model by Eqs. (11) and

(12), respectively. The **F** matrix is named the *Evolution matrix*, which is obtained by the discretization from the Finite Difference Method, **H** is the *Observation matrix* and $\mathbf{u}_{\mathrm{k}}$ is the input vector, the same defined in Eq. (8).

$$\mathbf{x}_{\mathrm{k}} = \mathbf{F}\mathbf{x}_{\mathrm{k\text{-}1}} + \mathbf{u}_{\mathrm{k}-1} + \mathbf{w}_{\mathrm{k}} \tag{11}$$

$$\mathbf{y}_{\mathrm{k}} = \mathbf{H}\mathbf{x}_{\mathrm{k}} + \mathbf{v}_{\mathrm{k}} \tag{12}$$

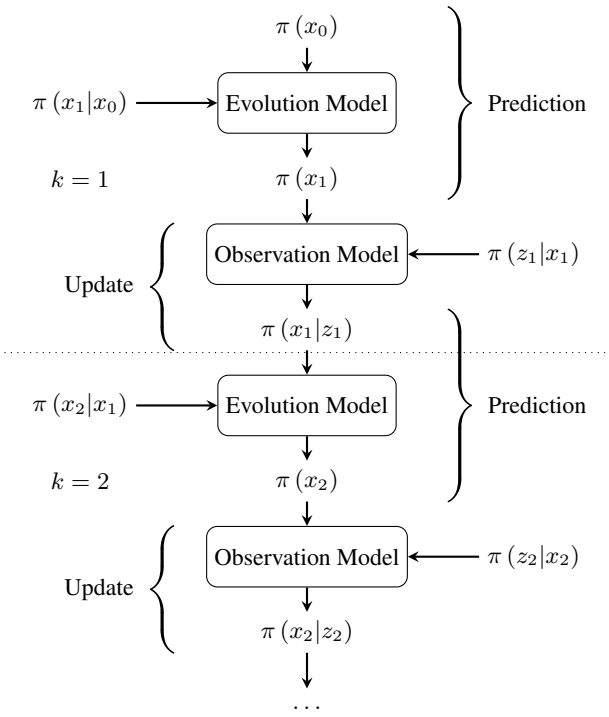


Figure 2. Flowchart for filtering problem (Ristic *et al.*, 2004).

To allow the simultaneous temperature and heat flux estimation, we adopt the *augmented vector* technique by assembling the temperature and heat flux values in a single state vector. In addition, the evolution model is considered as a *random walk model*. We consequently can write the augmented state vector and the heat flux evolution model as in Eqs. (13) and (14), respectively. It should be remarked that the parameter $\sigma_{\mathrm{rw}}$ is the standard deviation of the heat flux and $\boldsymbol{\omega}$ is a random standard Gaussian vector. High values for $\sigma_{\mathrm{rw}}$ admit a higher range of heat flux estimation.

$$\mathbf{x}_{\mathrm{aug}}\,(t) = \begin{bmatrix} \mathbf{x}_{\mathrm{T}}\,(t) \\ \mathbf{x}_{\mathrm{q}}\,(t) \end{bmatrix} \tag{13}$$

$$\mathbf{q}_{\mathrm{k}} = \mathbf{q}_{\mathrm{k}-1} + \sigma_{\mathrm{rw}}\boldsymbol{\omega} \tag{14}$$

Recalling that M is the total nodes on the space discretization, we can therefore define **F** (dimension of 2Mx2M), **H** (dimension Mx2M) and **u** (dimension of 2Mx1) by Eq. (15) - (17), respectively. On these equations, **0** and **I** are the *zero* and *identity* matrices, respectively.

$$\mathbf{F} = \begin{bmatrix} \mathbf{J}_{\mathrm{M\ x\ M}} & \alpha\Delta t C_1\ \mathbf{I}_{\mathrm{M\ x\ M}} \\ \mathbf{0}_{\mathrm{M\ x\ M}} & \mathbf{I}_{\mathrm{M\ x\ M}} \end{bmatrix} \tag{15}$$

$$\mathbf{H} = \begin{bmatrix} \mathbf{I}_{\mathrm{M\ x\ M}} & \mathbf{0}_{\mathrm{M\ x\ M}} \end{bmatrix} \tag{16}$$

$$\mathbf{u} = \begin{bmatrix} \mathbf{s}_{\mathrm{M\ x\ 1}} \\ \mathbf{0}_{\mathrm{M\ x\ 1}} \end{bmatrix} \tag{17}$$

Finally, we can write the sequential estimation for the described inverse problem with Kalman filter by Eqs. (18) - (22). The matrix $\mathbf{K}_{\mathrm{k}}$ is known as *Kalman gain* and it performs the weight correction, correlating the predicted and measurement vectors.

- Prediction:

$$\mathbf{x}_{\mathrm{k}}^{-} = \mathbf{F}\hat{\mathbf{x}}_{\mathrm{k}-1} + \mathbf{u}_{\mathrm{k}-1} \tag{18}$$

$$\mathbf{P}_{k}^{-} = \mathbf{F}\mathbf{P}_{\mathrm{k}-1}\mathbf{F}^{\mathrm{T}} + \mathbf{Q}_{\text{k-1}} \tag{19}$$

- Update:

$$\mathbf{K}_{\mathrm{k}} = \mathbf{P}_{\mathrm{k}}^{-}\mathbf{H}^{\mathrm{T}}\mathbf{S}_{\mathrm{k}}^{-1} \tag{20}$$

$$\hat{\mathbf{x}}_{\mathrm{k}} = \mathbf{x}_{\mathrm{k}}^{-} + \mathbf{K}_{\mathrm{k}}\left(\mathbf{z}_{\mathrm{k}} - \mathbf{H}\mathbf{x}_{\mathrm{k}}^{-}\right) \tag{21}$$

$$\mathbf{P}_{\mathrm{k}} = \left(\mathbf{I} - \mathbf{K}_{\mathrm{k}}\mathbf{H}\right)\mathbf{P}_{\mathrm{k}}^{-} \tag{22}$$

$$\mathbf{S}_{\mathrm{k}} = \left(\mathbf{H}\mathbf{P}_{\mathrm{k}}^{-}\mathbf{H}^{T} + \mathbf{R}_{\mathrm{k}}\right) \tag{23}$$

As stated in Özisik and Orlande (2000), it is well known that inverse heat conduction problems are ill-posed problems. Also, since we are estimating a large number of parameters, i.e. the heat flux at all measurement points (which match with those from the Finite Difference Method), the inverse problem can present instabilities due to the existence of measurement errors. To reduce such instabilities, a *regularization* technique should be used (Özisik and Orlande, 2000). On Kalman filter, such instability will be produced in Eq. (20) by the inversion of the Kalman gain matrix $\mathbf{K}_{\mathrm{k}}$ (Schulze *et al.*, 2009). So, we can include the Tikhonov regularization by the rewriting the Kalman gain by Eqs. (24) and (25), where $\lambda$ represents the *regularization parameter*.

$$\tilde{\mathbf{K}}_{\mathrm{k}} = \mathbf{P}_{\mathrm{k}}\mathbf{H}^{\mathrm{T}}\tilde{\mathbf{S}}^{-1} \tag{24}$$

$$\tilde{\mathbf{S}}^{-1} = \left(\mathbf{S}^{\mathrm{T}}\mathbf{S} + \lambda\mathbf{I}\right)^{-1}\mathbf{S}^{\mathrm{T}} \tag{25}$$

## 4. RESULTS AND DISCUSSIONS

Once both forward and inverse problems are defined, the current section presents the results obtained by the Kalman filter for the internal heat flux estimation. We consider temperature measurement available on the external wall surface of the adiabatic section on an PHP, simulating an Infrared Camera device for temperature acquisition. The values of geometrical and thermal properties used in this work are considered to be available, presented in Tab. 1, and they will be used in both forward and inverse problems.

Table 1. Physical and geometric properties considered in this work (Pagliarini *et al.*, 2021).

| Property | Value | Unit |
|---|---|---|
| $\rho$ | 2700 | [kg / m³] |
| $c_p$ | 900 | [kJ / kg K] |
| $k$ | 201 | [W / m K] |
| $h_\infty$ | 10 | [W / m² K] |
| $T_\infty$ | 22 | [ºC] |
| $r_{\mathrm{i}}$ | 0.0015 | [m] |
| $r_{\mathrm{o}}$ | 0.0025 | [m] |
| $L$ | 0.1 | [m] |

The heat flux function $\mathrm{q}\left(z,t\right)$ is considered to be known on the forward problem in order to obtain the synthetic temperature measurement. Thus, the heat flux function is defined according to Pagliarini *et al.* (2021) work and it is written in Eq. (26). The parameter $p$ represents the frequency oscillation on time for the heat flux, while $A$ represents the heat flux amplitude. We considered the values of $1.2$, $1.8$ and $2.4$ for $p$ and $2000$ and $4000$ W/m² for $A$ (Pagliarini *et al.*, 2021). The simulated temperature measurements are obtained by the forward solution of the heat conduction problem described on the previous section, with total time of experiment of 10s. Uncorrelated white Gaussian random sequence with known standard deviation $\sigma_{\text{meas}}$, see Eq. (27), are included to those synthetic data, where $\boldsymbol{\nu}$ is the random standard Gaussian vector. Three different measurement noises were considered: 0.01, 0.06 and 0.1 °C. To avoid the inverse crime (Kaipio and Somersalo, 2004), the forward problem was solved using a fine space and time mesh discretization when compared with the inverse problem. The space and time discretization for the forward problem is set with $N_z = 201$ nodes ($\Delta x = 0.005$m) and $\Delta t = 0.0002$s, respectively, where the temperature measurements are considered to be available with a frequency of $50$Hz (every $\Delta t_{\text{meas}} = 0.2$s) and on space with $\Delta z_{\text{meas}} = 1$mm (Pagliarini *et al.*, 2021).

$$\mathrm{q}\left(z,t\right) = A\cos\left(p\pi t\right)\left(1 + \frac{z}{8}L\right) \tag{26}$$

$$\mathbf{T}_{\text{meas}} = \mathbf{T}_{\text{exact}} + \sigma_{\text{meas}}\boldsymbol{\nu} \tag{27}$$

The Kalman Filter estimation accuracy is analysed by Eq. (28), as calculated according to Pagliarini *et al.* (2021). Here, $\text{N}_{\text{time}}$ and $\text{N}_{\text{space}}$ represents the total number of measurement along experiment time and along the total number of measurement points on space, respectively.

$$\text{E}_{\text{heat estimated}} = \frac{\|\text{q}_{\text{estimated}} - \text{q}_{\text{exact}}\|_2}{A\sqrt{\text{N}_{\text{time}}\text{N}_{\text{space}}}} \tag{28}$$

The code was implemented for both forward and inverse problems on MATLAB®. The computer used for the simulations was an Intel(R) Core(TM) i5-8265U CPU @ 1.60GHz - 1.80 GHz, 8Gb RAM running Windows 10. For the proposed experiment, the calculation time for the Kalman filter estimation was in average 6.73s, with maximum of 7.64s, requiring less time for calculation than the total time of experiment (10s), making possible therefore the use on real-time.

During the simulation tests, the parameter $\sigma_{\text{rw}}$, from Eq. (14), performed an important role on heat flux estimation on Kalman filter. Briefly, when $\sigma_{\text{rw}}$ decreases, the smoothness for the heat flux estimation is achieved, whereas the estimation was delayed with the respect to exact heat flux data. Otherwise, when $\sigma_{\text{rw}}$ increases, the response delay was reduced, but on the other hand it affected the smoothness of heat flux estimation. Thus, a trial and error procedure was crucial to obtain the better $\sigma_{\text{rw}}$. This parameter therefore was chosen for each case by evaluating the estimated error from Eq. (28) and by graphical visualization.

We present the results obtained for each case with the corresponding measurement error in Tab. 2. Regarding the error for the estimated heat flux, we can see that for all cases the Tikhonov regularization reduced the error between the estimated and exact heat flux. It can be seen also that the use of the regularization on the highest value of measurement error was crucial, showing a high reduction on error in all cases. Moreover, the value of $\sigma_{\text{rw}}$ needed to be incremented when the regularization was performed.

| Case | | | Without Tikhonov | | With Tikhonov | | |
|---|---|---|---|---|---|---|---|
| $A$ | $p$ | $\sigma_{meas}$ | $\text{E}_{\text{heat estimated}}$ | $\sigma_{\text{rw}}$ | $\text{E}_{\text{heat estimated}}$ | $\text{E}_{\text{heat estimated}}$ | $\lambda_{\text{Tikhonov}}$ |
| 2000 | 1.2 | 0.01 | 0.564 | 11 | 0.433 | 600 | $10^{-2}$ |
| | | 0.06 | 1.389 | 20 | 0.93 | 650 | 1 |
| | | 0.1 | 1.961 | 30 | 1.047 | 750 | 10 |
| | 1.8 | 0.01 | 0.702 | 12.5 | 0.530 | 750 | $10^{-2}$ |
| | | 0.06 | 1.665 | 22.5 | 1.193 | 800 | 1 |
| | | 0.1 | 2.228 | 32.5 | 1.406 | 1000 | 10 |
| | 2.4 | 0.01 | 0.821 | 15 | 0.617 | 800 | $10^{-2}$ |
| | | 0.06 | 1.916 | 23.5 | 1.393 | 850 | 1 |
| | | 0.1 | 2.460 | 34 | 1.6738 | 1100 | 10 |
| 4000 | 1.2 | 0.01 | 0.406 | 15 | 0.317 | 650 | $10^{-2}$ |
| | | 0.06 | 0.983 | 17.5 | 0.697 | 900 | 1 |
| | | 0.1 | 1.231 | 33 | 0.824 | 1050 | 10 |
| | 1.8 | 0.01 | 0.531 | 16.5 | 0.398 | 800 | $10^{-2}$ |
| | | 0.06 | 1.222 | 26.5 | 0.876 | 950 | 1 |
| | | 0.1 | 1.526 | 41.5 | 1.071 | 1200 | 10 |
| | 2.4 | 0.01 | 0.614 | 21 | 0.456 | 1000 | $10^{-2}$ |
| | | 0.06 | 1.4352 | 33 | 1.039 | 1250 | 1 |
| | | 0.1 | 1.773 | 46.5 | 1.285 | 1500 | 10 |

Table 2. Results obtained of estimation errors for the different heat flux cases.

Keeping in regard the results in Tab. 2, we can observe that the parameter $A$, which represents the amplitude of the heat flux, provides a high influence on the estimation. We can notice that for cases when $A = 4000$ W/m² the error was lower when comparing to those obtained when $A = 2000$ W/m². The discussion regarding the amplitude value needs to take into account that the maximum temperature difference between two time steps of measurement for the exact solution is about 0.043°C for $A = 2000$ W/m² and 0.086°C for $A = 4000$ W/m². So, the measurement noises can be greater than the maximal temperature difference, compromising the heat flux estimation. Further, we can see that when we increase the value of the frequency parameter $p$, the estimate error increases. The oscillation behavior of the heat flux is discussed on inverse heat problems (Beck *et al.*, 1985), showing that this frequency influences on the estimation results. To obtain a better estimate, the parameter $\sigma_{rw}$ must be increased to reduce the lagging problem.

Since we are dealing with a large number of estimation data along time, we present some graphical results to demonstrate the influence of the parameter $\sigma_{\text{rw}}$ and Tikhonov regularization. We present on Figures 3 to 10 the results obtained.

We can observe in Fig. 3, 4, 7 and 8 that the estimation provided a good matching with the exact solution, where in all cases the measurement noise considered was the smaller one. When analysing Figs. 5, 7, 9 and 10, where the larger value of measurement error was assumed, we can see that the result was highly influenced by this noise. However, we can see that the Tikhonov regularization provided an important influence to smooth the solution, producing less unstable results. When we compare the results obtained for the cases with $A = 4000$ W/m² with the cases with $A = 2000$ W/m², we can see that for high values of this parameter we achieve a more accurate matching with the exact solution. Furthermore, when higher value for the parameter $p$ is considered, a lagging problem can be observed. This can be seen by comparing the results in Fig. 3 and 4 with the results in Fig. 7 and 8. This phenomenon can be better observed when the transient results are regarded.

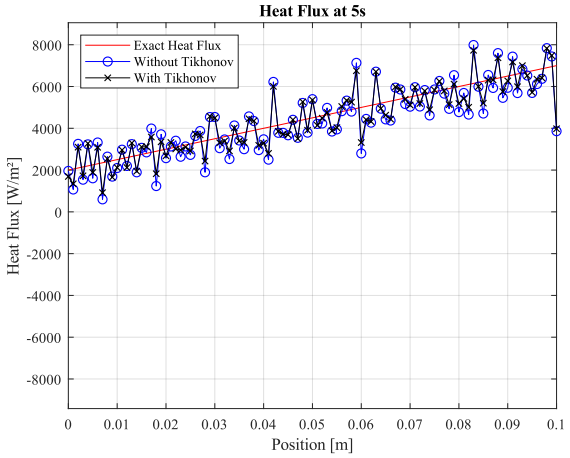


Figure 3. Result obtained for heat flux estimation for the case with $A = 2000$ W/m², $p = 1.2$ and $\sigma_{\text{meas}} = 0.01$ºC at 5s of experiment.

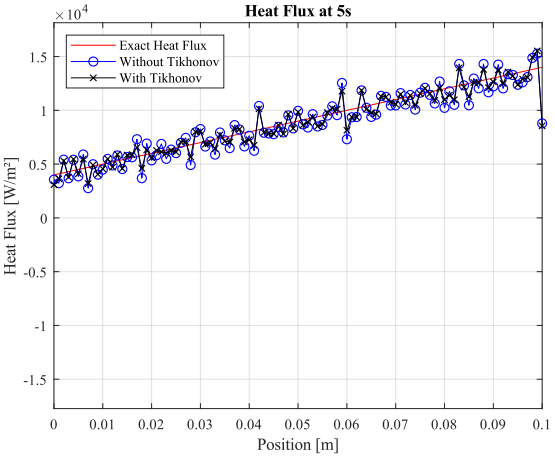


Figure 4. Result obtained for heat flux estimation for the case with $A = 4000$ W/m², $p = 1.2$ and $\sigma_{\text{meas}} = 0.01$ºC at 5s of experiment.

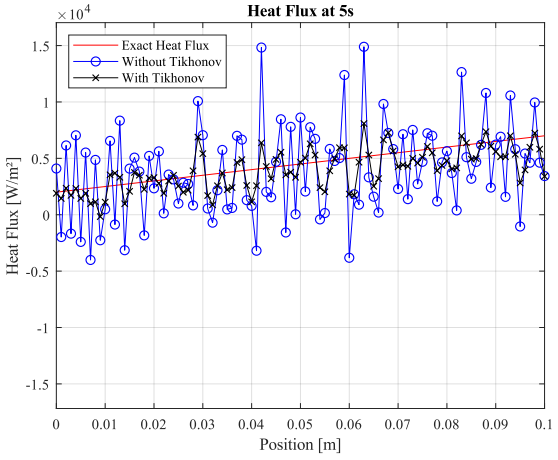


Figure 5. Result obtained for heat flux estimation for the case with $A = 2000$ W/m², $p = 1.2$ and $\sigma_{\text{meas}} = 0.1$ºC at 5s of experiment.

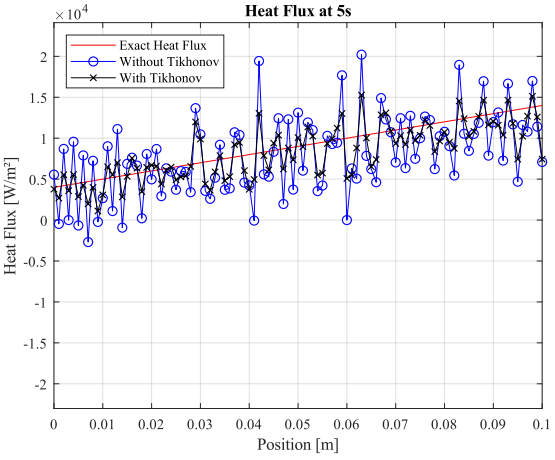


Figure 6. Result obtained for heat flux estimation for the case with $A = 4000$ W/m², $p = 1.2$ and $\sigma_{\text{meas}} = 0.1$ºC at 5s of experiment.

## 5. CONCLUSIONS

In this work, the Kalman filter is applied to estimate the heat flux between the working fluid and tube wall on Pulsating Heat Pipes. Synthetic data for temperature was used to evaluate the potential of Kalman filter to the proposed problem formulation. We compared three different measurement noises: 0.01, 0.06 and 0,1ºC. As expected, when the measurement noise increase, the filter accuracy to match the exact and estimated heat fluxes was compromised. Tikhonov regularization was applied on the Kalman gain matrix inversion to reduce instabilities on estimation accuracy along time, providing an improvement on estimation. The random walk parameter for the heat flux estimation demanded to be tuned for each case, where high values reduced the response delay produced by the measurement error. However, by increasing the

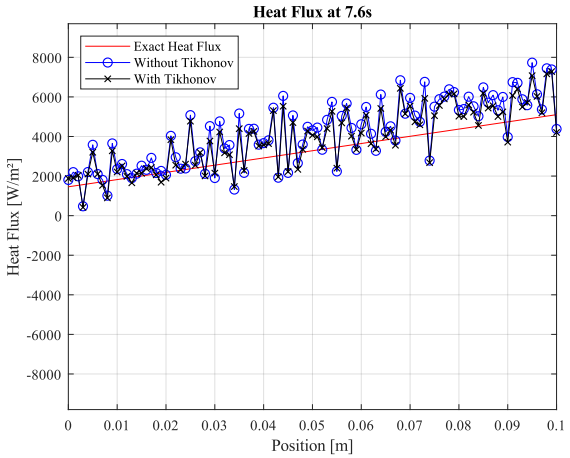


Figure 7. Result obtained for heat flux estimation for the case with $A = 2000$ W/m², $p = 2.4$ and $\sigma_{\text{meas}} = 0.01$ºC at 7.6s of experiment.

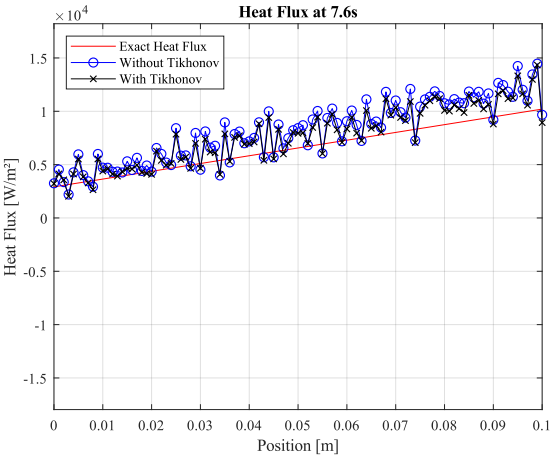


Figure 8. Result obtained for heat flux estimation for the case with $A = 4000$ W/m², $p = 2.4$ and $\sigma_{\text{meas}} = 0.01$ºC at 7.6s of experiment.

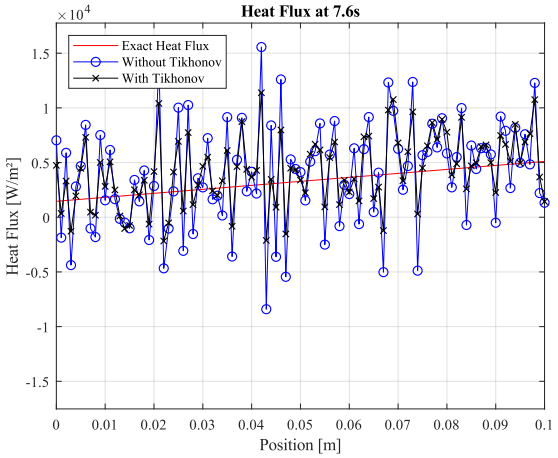


Figure 9. Result obtained for heat flux estimation for the case with $A = 2000$ W/m², $p = 2.4$ and $\sigma_{\text{meas}} = 0.1$ºC at 7.6s of experiment.

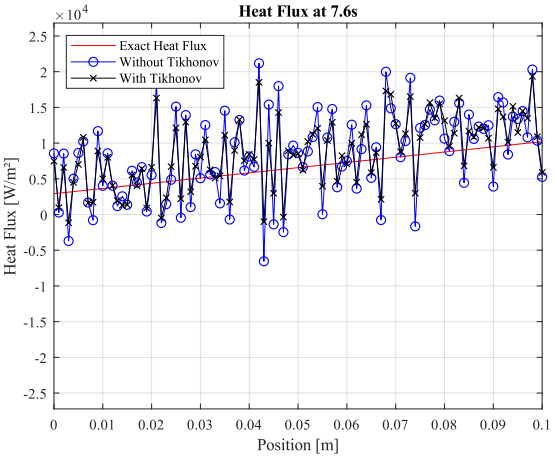


Figure 10. Result obtained for heat flux estimation for the case with $A = 4000$ W/m², $p = 2.4$ and $\sigma_{\text{meas}} = 0.1$ºC at 7.6s of experiment.

measurement noise value, the accuracy was affected. So, a trial and error procedure was necessary to observe precisely its influence, where it was noticed that for high values of frequency of $p$, it was necessary higher values for $\sigma_{\text{rw}}$, as well when observing the amplitude $A$.

The Kalman filter provided good results when comparing to the exact data, being an attractive tool for the proposal application since its implementation is considerably simple and the real-time was achieved since the time of experiment was lower than the calculation time. The application of Kalman filter should be analysed on further works with different heat flux functions, as well with real experimental data.

## 6. ACKNOWLEDGEMENTS

This paper was partially funded by the following Brazilian agencies: CNPq (Conselho Nacional para o Desenvolvimento Científico e Tecnoloógico), FAPERJ (Rio de Janeiro State Agency for Research) and ANP-PRH8 (Brazilian National Agency for Oil, Gas and BioFuels – Human Research Program number 8). The financial support and hospitality offered by Università degli Studi di Parma was also fundamental to this research.

## 7. REFERENCES

Bastakoti, D., Zhang, H., Li, D., Cai, W. and Li, F., 2018. "An overview on the developing trend of pulsating heat pipe and its performance". *Applied Thermal Engineering*, Vol. 141, pp. 305–322.

Beck, J., Jr, S., Blackwell, B., Clair, C. and Clair, C., 1985. *Inverse Heat Conduction: Ill-Posed Problems*. Wiley-

Interscience publication. Wiley.

Cattani, L., Mangini, D., Bozzoli, F., Pietrasanta, L., Miche, N., Mameli, M., Filippeschi, S., Rainieri, S. and Marengo, M., 2019. "An original look into pulsating heat pipes: Inverse heat conduction approach for assessing the thermal behaviour". *Thermal Science and Engineering Progress*, Vol. 10, pp. 317–326.

Daouas, N. and Radhouani, M., 2000. "Version étendue du filtre de kalman discret appliquée à un problème inverse de conduction de chaleur non linéaire". *International Journal of Thermal Sciences*, Vol. 39, pp. 191–212.

Han, X., Wang, X., Zheng, H., Xu, X. and Chen, G., 2016. "Review of the development of pulsating heat pipe for heat dissipation". *Renewable and Sustainable energy Reviews*, Vol. 59, pp. 692–709.

Kaipio, J.P. and Somersalo, E., 2004. *Statistical and Computational Inverse Problems*, Vol. 160 of *Applied Mathematical Sciences*. Springer New York, NY.

Marengo, M. and Nikolayev, V.S., 2018. *Pulsating Heat Pipes: Experimental Analysis, Design and Applications*, World Scientific, chapter Chapter 1, pp. 1–62.

Orlande, H.R.B., Colaço, M.J., Dulikravich, G.S., Vianna, F., Silva, W.B., Fonseca, H.M. and Fudym, O., 2012. "State estimation problems in heat transfer". *International Journal of Uncertainty Quantification*, Vol. 2, pp. 239–258.

Orlande, H.R.B., Dulikravich, G.S. and Colaço, M.J., 2008. "Application of bayesian filters to heat conduction problems". In *EngOpt 2008 - International Conference on Engineering Optimization*. Rio de Janeiro, Brazil.

Pacheco, C.C., Orlande, H.R.B., Colaço, M.J. and Dulikravich, G.S., 2014. "Identification of a position and time dependent heat flux using the kalman filter and improved lumped analysis in heat conduction". In *5th International Conference on Computational Methods (ICCM2014)*. Cambridge, England.

Pagliarini, L., Cattani, L., Bozzoli, F., Mameli, M., Filippeschi, S., Rainieri, S. and Marengo, M., 2021. "Thermal characterization of a multi-turn pulsating heat pipe in microgravity conditions: Statistical approach to the local wall-to-fluid heat flux". *International Journal of Heat and Mass Transfer*, Vol. 169, p. 120930.

Ristic, B., Arulampalam, S. and Gordon, N., 2004. *Beyond the Kalman Filter: Particle Filters for Tracking Applications*. John Wiley & Sons, New Jersey, 2nd edition.

Schulze, W., Farina, D., Jiang, Y. and Dössel, O., 2009. "A kalman filter with integrated tikhonov-regularization to solve the inverse problem of electrocardiography". In *International Federation for Medical and Biological Engineering (IFMBE)*. Berlin, Heidelberg, pp. 821–824.

Wang, X., Zhang, D. and Zhang, L., 2020. "Estimation of moving heat source for an instantaneous three-dimensional heat transfer system based on step-renewed kalman filter". *International Journal of Heat and Mass Transfer*, Vol. 163, p. 120435.

Özisik, M.N. and Orlande, H.R.B., 2000. *Inverse Heat Transfer: Fundamentals and Applications*. Taylor & Francis, New York, USA, 1st edition.

Özisik, M.N., Orlande, H.R.B., Colaço, M.J. and Cotta, R.M., 2017. *Finite Difference Methods in Heat Transfer*. Heat Transfer. CRC Press.

## 8. RESPONSIBILITY NOTICE

The authors are solely responsible for the printed material included in this paper.